The EMBO Journal Vol. 1 No. 1, pp.99–105, 1982

Point mutations change the thermal denaturation profile of a short DNA fragment containing the lactose control elements. Comparison between experiment and theory

F. Schaeffer*, A. Kolb, and H. Buc

Institut Pasteur, 75724 Paris cedex 15, France

Communicated by H. Buc
Received on 15 December 1981

To understand the denaturation process of short DNA segments we have chosen a 203-base pair (bp) restriction fragment containing the lactose control region. A steady decrease in GC content exists between its *i* proximal and *z* proximal ends. We confirm that this fragment melts at low salt in two subtransitions. A GC to AT mutation in the AT-rich region (mutation UV5) increases the number of denatured base pairs in the first subtransition and decreases the cooperativity of the melting process. A GC to AT mutation in the GC-rich region (mutation L8) decreases the number of denatured base pairs in the first subtransition and increases the cooperativity. These mutations induce the same shift in the temperature of half denaturation. The effects of both mutations are additive. A short deletion at the *z* end of the fragment affects only the first subtransition. When four GC pairs are added to both ends, the fragment melts in one transition. Comparison with the results obtained with a larger 789-bp *lac* fragment reveals strong end effects on base pair stability and suggests that denaturation of the 203-bp fragment proceeds unidirectionally from the *z* end. Good agreement is shown with the predictions made with the "zipper model" of Crothers *et al.* (1965).

Key words: lactose promoter/DNA melting/point mutations

Introduction

Theoretical studies of the thermal denaturation process of DNA have a high predictive power which for a long time could not be efficiently challenged by current experimental methods. The development of more sensitive spectrophotometers, coupled with the availability of large quantities of pure DNA fragments of known sequence (Tiollais *et al.*, 1974; Hardies and Wells, 1979) allow critical analysis of the theoretical predictions (for review see Wada *et al.*, 1980). For sometime we have focused our attention on a specific sequence, the regulatory region of the wild-type lactose operon (Schaeffer *et al.*, 1978). We have isolated this sequence on a 203-base pair (bp) restriction fragment for which both experimental and theoretical melting profiles have been extensively studied (Hillen *et al.*, 1981; Benight *et al.*, 1981). We have analysed how the denaturation profile of the wild-type 203-bp fragment is modified by single GC to AT changes at different points in the sequence. We have also examined the effects of short deletions or insertions introduced at crucial positions in this sequence and the effects of inserting this sequence in a larger 789-bp DNA fragment. The seven DNA fragments used in this study are described in Figure 1 where the changes in primary structure are localized with respect to the genetic map.

The wild-type (WT) fragment was selected because of its physiological interest and because of the particular distribution of GC pairs along the sequence, analysed statistically in Figure 2. Except for the first 13 bp, the *i* proximal end is GC rich. There is a steady decrease in the mean GC content between bp 35 and bp 179, and the sequence covering the last 24 bp, containing the start of the *lac z* gene, is relatively GC rich. The UV5 and L8 mutations are located far from the ends of the fragment. They cause the same net change in GC content but the L8 mutation is located in the GC-rich region whereas the UV5 mutation is in the AT-rich region.

Three modifications have been introduced to test the influence of end effects on base pair stability inside the 203-bp fragment. In the 211-bp L8UV5 fragment both ends were made more GC rich. In the 193-bp L8+ fragment a short deletion was introduced at the *z* proximal end. Finally a 789-bp fragment was studied. In this longer fragment the 203-bp sequence is isolated between two GC-rich regions (cf. inset of Figure 2).

We have investigated the following: (i) is the shape of the differential melting curve of the 203-bp WT fragment sensitive to a single GC to AT change and if so, to its location in the sequence?; (ii) how does the double perturbation introduced in the L8UV5 fragment compare with the changes due to each separate mutation L8 and UV5?; and (iii) what are the effects of end modifications on the melting process of 203-bp fragment?

The ultimate goal is to determine how the thermal stability of the base pairs of the *lac* promoter sequence changes when point mutations which *in vivo* alter the level of transcription of this operon are introduced in the sequence (the teleostability phenomenon, Dickson *et al.*, 1975).

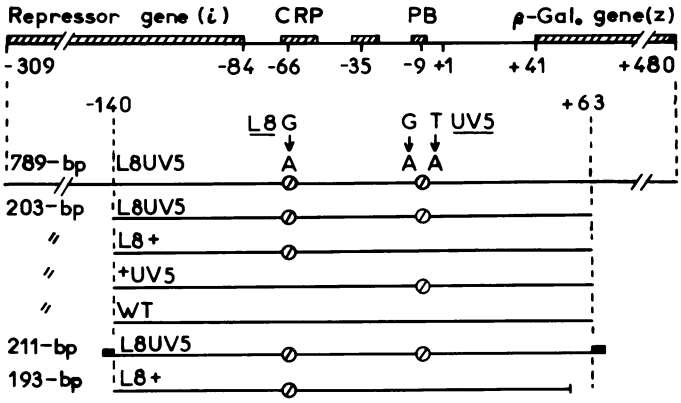

Fig. 1. The 789-, 211-, 203- and 193-bp fragments containing the regulatory region of the lactose operon. The genetic map shows the end of the *i* gene, the beginning of the *z* gene, the binding site of the CRP-cAMP complex, the RNA polymerase recognition regions (around −35 and −10) of the promoter sequence together with the location of the L8 (−66) and UV5 (−8, −9) point mutations. The numbering refers to the lactose mRNA start at +1. L8UV5 is a double mutant. The L8 mutation renders the lac promoter CRP-insensitive *in vivo* (Ippen *et al.*, 1968). The UV5 promoter is a strong "up" promoter in which the initiation of transcription is efficient in the absence of CRP (Silverstone *et al.*, 1970). WT refers to the sequence of the wild-type promoter, L8+ and +UV5 to the sequence bearing the single L8 or UV5 mutations. The 203-bp fragment is contained in the 789-bp fragment. The 211-bp fragment corresponds to the 203-bp L8UV5 sequence lengthened at both ends by four GC pairs. The 193-bp L8 + fragment results from a deletion of 13 bp between +49 and +61 followed by the insertion at +49 of the trinucleotide ATC.

*To whom reprint requests should be sent.

 0261-4189/82/0101-0099$2.00/0

Results

The melting process of the 203-bp fragment and the effects of internal sequence modifications: the L8 and UV5 mutations

In Figure 3 we compare the melting profile of the 203-bp WT fragment with those obtained with the L8+, +UV5, and L8UV5 fragments. Relevant data are compiled in Table I.

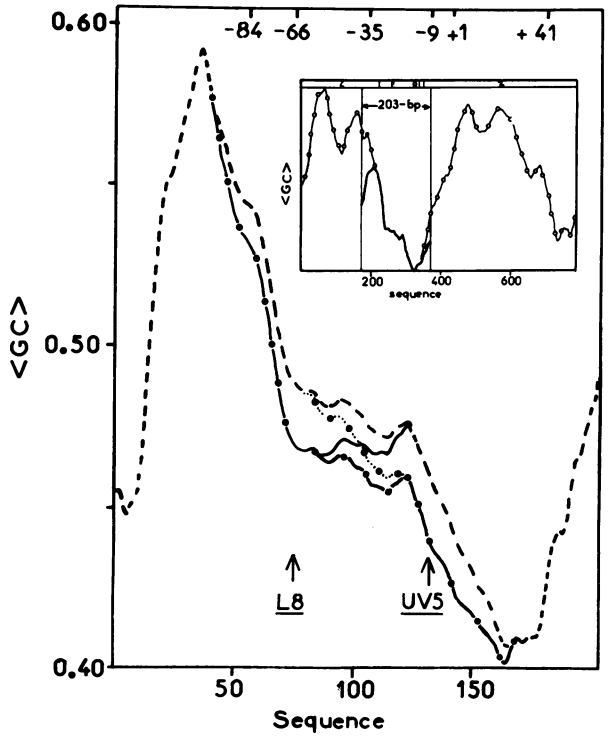

Fig. 2. An analysis of the mean value of the local percentage in GC content as a function of base position in the 203-bp WT, L8+, +UV5 and L8UV5 sequences (the figure), the 203- and 789-bp L8UV5 sequences (the inset). **Figure**: the 203-bp sequences L8UV5 (●—●), L8+ (—), +UV5 (●...●) and WT (– –). **Inset**: the 789-bp (○—○), 203-bp (—) L8UV5 sequences. **Figure**: the curves at both ends (– –) are identical for all four fragments. The numbering at the top of the figure is as in Figure 1. The sequence is numbered from left to right. For each base i ($0 \leq i \leq 203$), all the sequences of L bases containing the i base were considered. The mean value for the GC content of each of these sequences thus calculated, is defined as the local GC content at base i. A single value of L, of the order of magnitude of the correlation length (Crothers, 1968, Poland and Scheraga, 1969) has been used here (L = 50). If base i is close to the ends of the fragment ($1 \leq i \leq 50$, $154 \leq i \leq 203$) the following procedure has been achieved: L is decreased from 50 to 25 as i decreases from 50 to 25 or increases from 153 to 178. For $i < 25$ or > 178, the sequence is symmetrically lengthened through a mirror placed at the ends and the calculation is performed as above. This classical procedure gives an even statistical weight to each base of the sequence. **Inset**: Computation was performed as in the figure, L being kept equal to 50.

The $T_{1/2}$ of the WT fragment is lowered by 0.2°C by either the L8 or the UV5 mutations and by twice this value by the double L8UV5 mutation. However, each mutation affects the shape of the asymmetrical melting curve of the WT fragment differently: the UV5 mutation affects mainly the beginning of the process, while the L8 mutation affects the middle and the end. At low temperature, when 10 ± 2 bp are open (as judged from the amount of hyperchromy) the +UV5 and L8UV5 curves separate from those of L8+ and WT. The separation of the L8UV5 curve from that of +UV5, as well as the L8+ curve from that of WT, takes place at higher temperatures when 25 ± 5 bp are open. Thus, a mutation located in the AT-rich region affects the melting process earlier than one located in the GC-rich region. The four curves order themselves in the series L8UV5, L8+, +UV5, and WT at the end of the process.

The cooperativity of the melting profile also depends strongly on the sequence. A very cooperative process is characterized by a high value of Y_m, a small difference be-

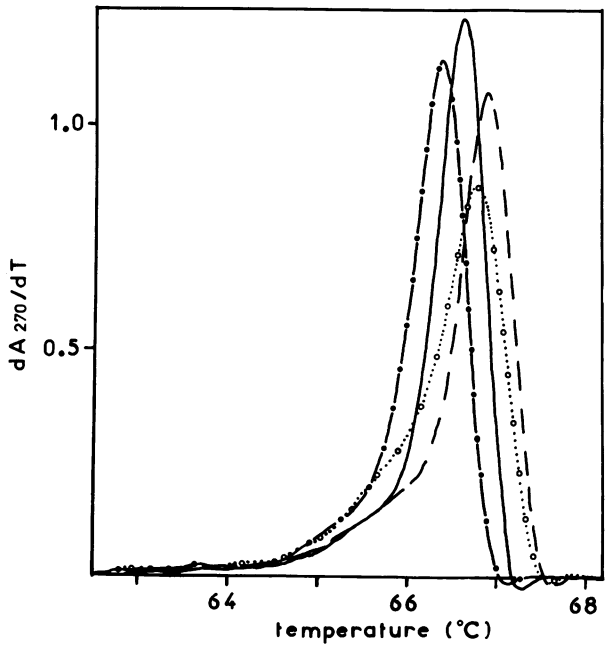

Fig. 3. Differential melting curves of the 203-bp fragments. L8UV5 (●—●), +UV5 (○...○) L8+ (—) and WT (– –). The vertical axis represents the derivative of the absorbance at 270 nm as a function of temperature, the total hyperchromicity being normalized to 1. Denaturation of all four fragments starts at 62.5 ± 0.20°C. The +UV5 and L8UV5 curves separate from the L8+ and WT at 64.5 ± 0.15°C. The L8UV5 curve separates from the +UV5 curve at 65.5 ± 0.10°C. The L8+ curve separates from the WT curve at 65.7 ± 0.10°C.

Table I. Some characteristics of the experimental differential melting profiles of the lactose fragments shown in Figures 3, 4, and 5.

Fragment	GC(%)	$T_{1/2}$(°C)	T_m (°)	$T_m - T_{1/2}$ (°C)	Y_m(A/C°)	$l_{1/2}$ (°C)	n (T_m)	m	n_1	n_2	n_3	n_4
203 bp WT	48.276	66.71	66.90	0.19	1.08	0.69	134	69	42	165	–	–
203 bp +UV5	47.783	66.51	66.76	0.25	0.87	0.88	141	62	49	154	–	–
203 bp L8+	47.783	66.52	66.61	0.09	1.24	0.64	128	75	24	179	–	–
203 bp L8UV5	47.290	66.30	66.36	0.07	1.15	0.69	128	75	24	179	–	–
211 bp L8UV5	49.282	66.66	66.69	0.03	1.27	0.68	124	87	–	211	–	–
193 bp L8+	48.186	66.61	66.62	0.01	1.30	0.60	120	73	15	178	–	–
789 bp L8UV5	54.246	71.00	–	–	–	–	–	–	70	36	274	409

$T_{1/2}$ and T_m are respectively the temperatures at which a fragment is half denatured and of the maximum Y_m of the derivative value. $l_{1/2}$ is the width of the peak at half height ($Y_m/2$).n_i, $n(T_m)$ and m are respectively the number of base pairs denatured in thermalite i, at T_m and from T_m to the end of the denaturation process.

tween T_m and $T_{1/2}$ and a sharp peak (small value of $l_{1/2}$). The transition is more cooperative for the L8+ fragment than for the WT fragment. In contrast, with the +UV5 fragment, the melting is less cooperative. The profile of the L8UV5 fragment is identical to that of the +UV5 fragment at the beginning of melting, but becomes as sharp as the profile of the L8+ fragment at the end of denaturation. These observations can be correlated with the distribution of GC pairs shown in Figure 2: the more regular the gradient in GC content, the less cooperative the melting process. Compared to the distribution of GC pairs in the WT sequence, the UV5 mutation makes the slope of the curve of Figure 2 nearly constant while the L8 mutation has the opposite effect. Note that the variations in the slope of the gradient in GC content are roughly the same for the WT and L8UV5 fragments.

Each asymmetrical melting profile in Figure 3 can be resolved into two subtransitions (thermalites in the terminology of Vizard and Ansevin, 1976), the shoulder on the low temperature side of the major peak and the major peak itself (see also Hardies *et al.*, 1979). The number of base pairs denatured in each thermalite (n_1 and n_2) together with that determined at the T_m ($n(T_m)$) are listed in Table I. With respect to the WT, the L8 mutation shifts the thermodynamic boundary between thermalites 1 and 2 towards lower temperatures thus decreasing n_1 by 18 bp and $n(T_m)$ by 6 bp (Table I). The UV5 mutation acts again in the opposite way, increasing n_1 and $n(T_m)$ by 7 bp each (Table I). The effect of the UV5 mutation is absent in the L8 background since the L8UV5 fragment is characterized by the same value of n_1 as the L8+ fragment.

We have examined whether the effects of the two mutations are additive. We compared the shape of the two curves obtained by adding the melting profiles of either the L8+ and +UV5 fragments or of the L8UV5 and WT. As the GC content of the L8UV5 and WT fragments is significantly different, one has to shift these curves on the temperature axis prior to summation in order to superimpose their $T_{1/2}$ values to the $T_{1/2}$ values of the L8+ and +UV5 fragments. Under these conditions the two sums are identical within experimental error (curves not shown), thus indicating that the effects of the two mutations L8 and UV5 are additive.

The effects of end modifications on the melting process of the 203-bp fragment: the 193-, 211-, and 789-bp fragments

The comparison between the melting profiles of the 193- and 203-bp L8+ fragments (Figure 4a and Table I) shows that the 10-bp deletion located at the *z* end of the 203-bp sequence alters only the first thermalite (n_1 is decreased by 9, the length of the deletion within experimental error). Thus, the *z* end of the 203-bp fragment melts in the first denaturation step. This deletion does not affect the location of the thermodynamic boundary between thermalites 1 and 2 as

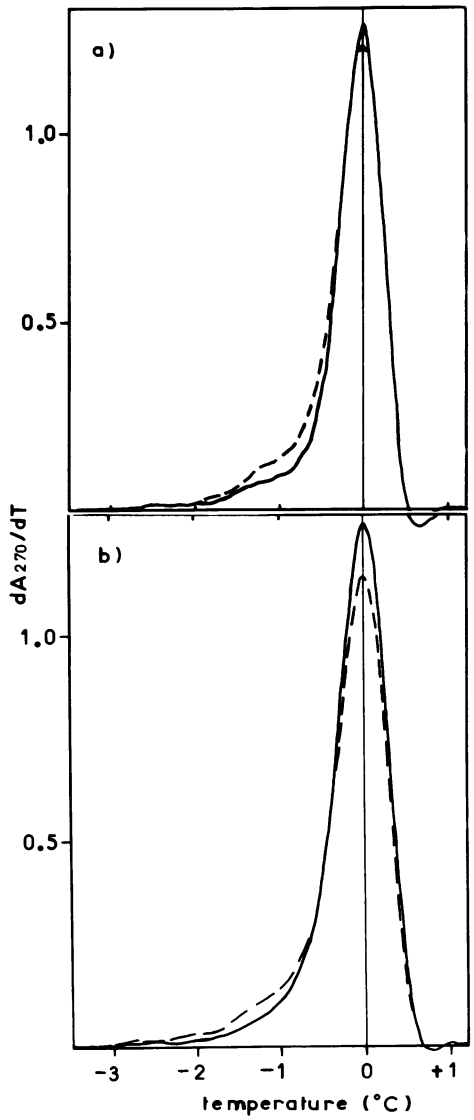

Fig. 4. Differential melting curves of the 193-bp L8+ and 211-bp L8UV5 fragments. Comparison between **a** the 193-bp (—) and 203-bp (– –) L8+ fragments, **b** the 211-bp (—) and 203-bp (– –) L8UV5 fragments. The vertical axis is as in Figure 3. The total hyperchromicity of each fragment is adjusted to the number of base pairs. The horizontal axis represents the displacement from T_m in °C.

Table II. Some characteristics of the theoretical differential melting curves calculated for the sequences studied by the "zipper model" of Crothers, Kallenbach, and Zimm (1965).

Fragment	$T_{1/2}$[MD](°C)	$T_{1/2}$ (°C)	Y_m(A/°C)	T_m (°C)	$l_{1/2}$ (°C)	$n(T_m)$	m	$T_m - T_{1/2}$ (°C)
203 bp WT	67.91	66.70	0.62	66.96	1.11	141	62	0.26
203 bp +UV5	67.71	66.45	0.55	66.76	1.33	141	62	0.31
203 bp L8+	67.71	66.45	0.66	66.66	1.08	135	68	0.21
203 bp L8UV5	65.51	66.20	0.61	66.40	1.23	135	68	0.20
211 bp L8UV5	68.33	66.55	0.93	66.60	0.95	120	91	0.05
193 bp L8+	67.87	66.50	0.65	66.65	1.05	125	68	0.15
789 bp L8UV5	70.36	70.93	–	–	–	–	–	–

$T_{1/2}$[MD] is the value of $T_{1/2}$ determined by the relation of Marmur and Doty corrected for ionic strength. Other parameters are as in Table I.

measured in number of denatured base pairs (n_2 remains constant).

The melting profile of the 211-bp L8UV5 fragment shows greater modifications (Figure 4b). Addition of four GC pairs to each end of the 203-bp L8UV5 fragment induces an increased cooperativity in the melting process. The differential melting curve of the 211-bp fragment is continuous from the beginning, no obvious disruption in the slope appearing on the low temperature side of the curve as with the other fragments. Therefore, the whole 211-bp sequence melts in one thermalite as if the thermodynamic boundary between thermalites 1 and 2 of the 203-bp sequence had vanished by the addition of the GC pairs.

The 789-bp L8UV5 fragment melts at a higher temperature than the 203-bp L8UV5 fragment and its melting profile displays four thermalites (Figure 5 and Table I). These results are in good agreement with those of Hardies *et al.* (1979). None of these thermalites can be identified as directly corresponding to the 203-bp sequence which must have been stabilized by the two GC-rich sequences mentioned in the **Introduction**. A complete analysis of the thermal behaviour of this 789-bp sequence will be given elsewhere.

$T_{1/2}$ analysis. One can compare to the experimental $T_{1/2}$ values those predicted by the relation of Marmur and Doty (1962) as revised by Schildkraut and Lifson (1965) for changes in ionic strength (see Tables I and II). First, it appears that the $T_{1/2}$ values of the four 203-bp, the 193-bp, and the 211-bp fragments are respectively 1.20°, 1.26°, and 1.67°C lower than the predicted values. These differences are significant enough for us to conclude that the 203-bp and related sequences are less resistant to heat denaturation than long molecules of the same GC content to which the relation of Marmur and Doty applies. On the contrary, this relation applies to the larger 789-bp fragment. Second, the relation of Marmur and Doty predicts precisely the differences in $T_{1/2}$ of the 203-bp sequences induced by the internal modifications L8 and UV5 (0.20°C and 0.40°C for the single and double mutations corresponding respectively to a change in GC content of 0.5 and 1%) but not the differences induced by modifications located at the ends, the predicted values being much higher than the experimental ones (for a change in GC content of 2% between the 211-bp and 203-bp L8UV5 fragments the predicted difference in $T_{1/2}$ value is of 0.81°C compared with observations of 0.36 ± 0.05°C, Table I). In other words, point mutations exert their full effect on the $T_{1/2}$ value of the 203-bp sequence only if they are located well within the fragment. There is a strong "end effect" inducing a preferential destabilization of base pairs near the termini.

Comparison between experiment and theory. The importance of end effects on the thermal stability of the 203-bp fragment (but not on the larger 789-bp fragment) prompted us to match our data with a simple two-state model which only takes into account melting from the ends: the "zipper model" formulated by Crothers *et al.* (1965).

In this model unbonded base pairs can exist only in a continuous chain at each end of the fragment and they are assigned a statistical weighting factor of unity. Bonded AT pairs are assigned a weighting factor s and bonded GC pairs a factor ks. Two experimental facts considerably restrain the choice of the constant k and the function $s(T)$. First, the change in $T_{1/2}$ with the GC content of long molecules has been measured under conditions similar to ours (Schildkraut and Lifson, 1965). Second, Sturtevant *et al.* (1958) have established a formula for the heat of formation of the helix from the coil. Since a short-chain model is envisaged, it is necessary to consider configurations in which the two strands come apart. The relevant dissociation constant is not precisely known but its order of magnitude can be deduced from theoretical and experimental considerations (see Crothers *et al.*, 1965).

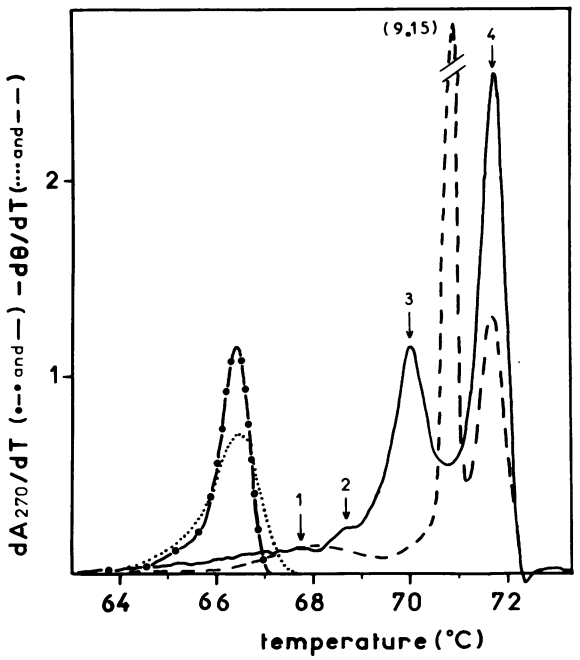

Fig. 5. Comparison between the experimental and predicted melting profiles of the 203- and 789-bp fragments using the zipper model of Crothers, Kallenbach and Zimm (1965). 203-bp sequence: experimental (●—●), calculated (...); 789-bp sequence: experimental (—), calculated (– –). θ, the fraction of bonded bases for all states was calculated using the following parameter values: ΔH = 15757-69 T cal/mol (equation derived from Sturtevant *et al.*, 1958), the stacking free energy ΔG_S = −7 kcal/mol of base pairs (Crothers and Zimm, 1964) T_A = 321°K the $T_{1/2}$ of AT pairs at 9.75 mM Na^+ salt (Schildkraut and Lifson, 1965), the average distance between bases in the single-strand DNA b = 10^{-7} cm. Simplification of the mathematical treatment of the zipper model leads to the determination of a mean value of k related to the content in GC of the sequence studied. However, k was adjusted to 4.82 to fit the theoretical $T_{1/2}$ value of the 203-bp WT sequence to its experimental value and kept constant for all other computations. To stay close to the experimental procedure a stepwise increment in temperature of 0.05°C was used. The calculation is performed for a sample of 0.6 ml with an A_{270} of 0.3.

The experimental and predicted melting profiles of the 203-bp and 789-bp L8UV5 fragments are shown in Figure 5. Comparison of these curves confirms the view that a model implying only denaturation from the ends fits well with the melting profile of the 203-bp fragment but not with that of the 789-bp fragment. Note, however, that for the 203-bp fragment the fit is not perfect, the experimental curve is more cooperative than the theoretical one (compare Y_m, $l_{1/2}$ and $T_m - T_{1/2}$ in Tables I and II). This difference will be fully analysed elsewhere.

The striking result of this analysis is that the simple model of Crothers *et al.* (1965) accounts for all the variations in $T_{1/2}$ as well as in the shape of the curves induced either by the internal mutations L8 and UV5 or by the modifications located at the ends of the 203-bp sequence (the 193- and 211-bp fragments). Figure 6 shows the predicted melting curves of the 203-bp sequences, either WT or with one or both of the L8 and UV5 mutations. These curves are asymmetric and (within small differences of the order of error in measurement), the values of Y_m, $T_m - T_{1/2}$, $l_{1/2}$, and $n(T_m)$ (Table II)

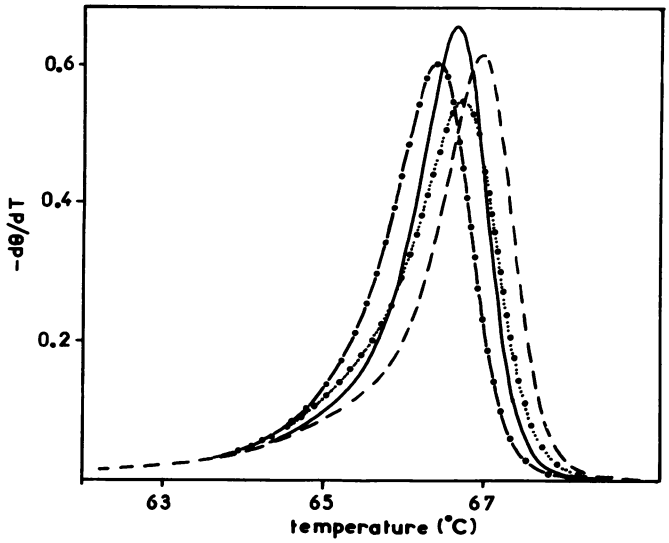

Fig. 6 Theoretical melting curves of the 203-bp sequences predicted by the model of Crothers *et al.* (1965). 203-bp L8UV5 (●—●), +UV5 (●...●), L8+ (—) and WT (– –). Computations are performed with the thermodynamic parameters given in legend of Figure 5. These curves present no obvious subdivision into two thermalites. This subdivision is clearly visible when higher k values are used in the computation.

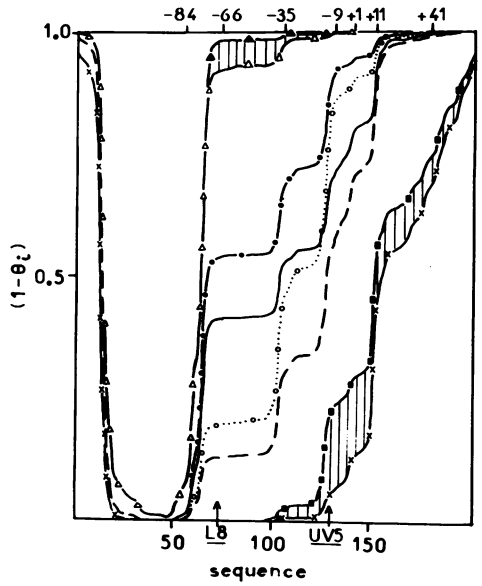

Fig. 7. Probability of opening of the base pairs of the 203-bp sequences at three temperatures. 66°C: WT and L8+ (x-x), +UV5 and L8UV5 (■—■); 68°C: WT (– –), +UV5 (○··○), L8+ (—), L8UV5 (●—●); 70°C: WT and +UV5 (△—△), L8+ and L8UV5 (▲—▲). The probability $1-\theta_i$ of base pair i being broken was determined when strand separation is forbidden (i.e., when at least one intact base pair remains) with the set of parameters of Figure 5. The area between the curve and the sequence axis is proportional to the number of denatured base pairs. The number of denatured base pairs on the i gene side is for the four sequences of 12, 13 and 15 bp at respectively, 66, 68 and 70°C. The numbers of denatured base pairs on the z gene side are respectively, for the WT, +UV5, L8+ and L8UV5 sequences of 38, 45, 38, 45 bp at 66°C; of 79, 92, 98, 112 bp at 68°C and of 137, 138, 140, 140 bp at 70°C. Base pair numbers are ±1 The three boundaries located at position −126, −76 and +11 define four areas corresponding for the WT sequence to $n_1(i)$ bp between the i end and position −126, $n_1(z)$ bp between the z end and position +11, n_2 bp between position +11 and −76 and n_3 bp between position −76 and −126.

order themselves respectively as the experimental values (Table I). These theoretical data corroborate the experimental observations that the melting process is most cooperative for the L8+ sequence and least cooperative for the +UV5 sequence. The asymmetry of the curves [measured by $n(T_m)$ and $T_m - T_{1/2}$, Table II] is, as observed experimentally (Table I), strongly affected by the presence of the L8 mutation.

Applied to the 193-bp L8+ and 211-bp L8UV5 sequences the model accounts also for the differences in the melting process of these two fragments with respect to the corresponding 203-bp L8+ or L8UV5 fragments (cf., Table II). The main characteristics of the theoretical curves are: for the 193-bp sequence, the decrease by 10 bp of $n(T_m)$ which is equal to the length of the deletion while m remains constant; for the 211-bp sequence an increase in cooperativity (Y_m is the largest) and a loss of the asymmetry of the main transition (between the 203- and 211-bp sequences the difference $T_m - T_{1/2}$ decreases by 0.15°C and m increases by 23 bp, Table II).

The prediction by the model of the $T_{1/2}$ values of the 193-bp and 211-bp fragments (Table II) confirms that, with short fragments, the observed variation from the $T_{1/2}$ values determined by the relation of Marmur and Doty is the result of destabilization due to end effects.

Discussion

When a very sensitive spectrophotometer is used to observe the thermal denaturation of purified DNA fragments of known sequence, it is easy to monitor the effect of single GC to AT mutations. Accurate measurement of the temperature (±0.002°C), reproducible determination of small absorbance changes (5 x 10^{-5} unit), and on-line treatment of the data (which are stored only when equilibrium is reached) are required to take full advantage of the method. This technique is sensitive to the position of the GC to AT transition in the sequence (Figure 3); therefore it has reached the level of analytical spectroscopy.

The comparison at low salt (10^{-2} N Na^+) of the melting profiles of the fragments listed on Figure 1 allows us to answer the questions listed in the introduction: (i) two point mutations and a short deletion affect different parts of the melting profile of the 203-bp fragment (Figures 3 and 4a). The analysis of these results suggest that denucleation proceeds from the z end towards the i end of the fragment; (ii) the pertubations induced in the denaturation process of the 203-bp fragment by the two-point mutations are additive; and (iii) lengthening the fragment at both ends (the 211- and 789-bp fragments, Figures 4b and 5) reveals that the 203-bp fragment is destabilized due to its short length.

These conclusions led us to analyse our data according to the "zipper model" of Crothers *et al.* (1965). This model makes use of a restricted number of parameters, the equilibrium constants for the nucleation (K) and elongation (s and ks) processes. Taking into account only melting from the ends, the model fits reasonably well with our data and accurately predicts the differences in the melting curve of the 203-bp fragment due to the small sequence modifications studied. The model fails in the case of the 789-bp fragment, where it is known that internal denucleation occurs (Patient *et al.*, 1979). Although the theory of Crothers *et al.* (1965) does not fully account for the cooperativity of the process (the 203-bp fragment in Figure 5), it can be considered as a good and reliable tool for short fragments. Our conclusion agrees well with the study of Benight *et al.* (1981) who, using a general loop entropy model including strand dissociation, concluded that denaturation of the 203-bp L8UV5 fragment occurs without formation of internal loops.

Theory predicts a drastic increase in the cooperativity of

the denaturation of short fragments due to strand dissociation (Crothers *et al.*, 1965; see also Hillen *et al.*, 1981). In Figure 7 we have computed the probability of opening each base pair of the 203-bp sequence either of WT or of the L8 or UV5 mutations under conditions where strand dissociation is forbidden. For a given sequence, comparison of the curves computed at three temperatures shows that except for the early melting of 12−15-bp at the *i* end, the denaturation is unidirectional, starting from the *z* end. The steepness of the function $1-\theta_i$ at certain points of the sequence reveals three main boundaries, located at position −126, −76, and +11. The experimental evidence for these boundaries − which should generate three thermalites corresponding respectively to $n_1(i) + n_1(z)$, n_2, and n_3 bp (cf., legend to Figure 7) − has been provided by Hillen *et al.* (1981) with the melting profile of a larger 301-bp fragment covering the same region. For the 203-bp sequence, theory predicts that, due to strand dissociation, only two thermalites are detectable (of n_1 (i) + n_1 (z) and $n_2 + n_3$ bp). In the case of the 211-bp sequence the first boundary located at +11 vanishes (theoretical curve not shown). This accounts for the observed denaturation of the 211-bp fragment in one thermalite.

At 68°C the four curves of Figure 7 show a series of plateaux, the largest one being located at the level of the cyclic AMP receptor-protein (CRP) site. These plateaux are separated by stepwise increments in probability located near the end of the *i* gene (−76), at the RNA polymerase recognition sites (−35 and −10), and at the center of the palindromic structure of the repressor site, the boundary at +11. Ordinates associated with the plateaux in the probability curves of the 203-bp sequences depend on the mutations but not the location of the boundaries. It remains to be seen whether the local denaturation which takes place at room temperature for the same fragments in the presence of RNA polymerase can be analysed in a similar way.

Materials and methods

Plasmid strains

Strain MM294 (Backman *et al.*, 1976) containing pMB9 plasmid with a 203-bp *lac* insert in the EcoRI site was a gift of Dr Ogata (Ogata and Gilbert, 1977). The 203-bp fragment carries either the WT *lac* promoter-operator region or the double mutant L8UV5. We constructed the L8+ and +UV5 fragments by cutting the two DNA fragments at their HpaII sites, resolving each mixture on a polyacrylamide gel, and religating the large 122-bp fragments carrying the CRP site to the smaller 81-bp fragment with the promoter-operator region. After addition of pBR322 plasmid DNA and cleavage by EcoRI restriction enzyme, the mixture was treated with T4 ligase. *Escherichia coli* (strain MM294) were transformed with the recombinant DNA and blue colonies carrying the recombinant plasmid were selected on plates containing tetracycline (20 μg/ml) and XG (5-chloro-4-bromo-3-indolyl-β-D-galactoside) (Miller, 1972). The *lac* fragments were sequenced according to Maxam and Gilbert (1977). A shorter recombinant was also obtained: the 193-bp *lac* fragment carrying the L8 mutation and described in Figure 1. Strain MM294 containing the pBR322 plasmid with a 211-bp *lac* fragment insertion in the EcoRI site was a gift of P. Charnay (Charnay *et al.*, 1978). Strain E7074 harboring the pMC1 plasmid with the 789-bp *lac* insert was from M. Calos (Calos, 1978).

DNA preparations

Plasmid DNAs were prepared according to Maquat and Reznikoff (1978) and purified with two cesium chloride-ethidium bromide gradients. After restriction, fragments were purified by zone centrifugation in a 5−20% sucrose gradient in 10 mM Tris-HCl, pH 8, 1 mM EDTA, 1 M NaCl. Fractions containing the fragments were ethanol precipitated, redissolved, dialysed against sodium citrate buffer (SSC) diluted 20-fold (7.5 mM NaCl, 0.75 mM trisodium citrate) and filtered through Millipore membrane filters (type HAWP 02500) previously washed with buffer.

DNA purity

DNA fragments were checked by gel electrophoresis on polyacrylamide and agarose gels. No contaminant band could be detected on gels after strand separation showing that no nick was present in the fragments (Hardies and Wells, 1979). EcoRI fragments could be ligated by T4 ligase into high molecular weight oligomers and recut by the restriction enzyme, indicating that the EcoRI termini were intact.

Measurements of absorption-temperature profiles

Thermal denaturation of DNA samples was performed with fully automated equipment through a stepwise temperature incrementation program which allows the recording of the stabilized absorbance values reached after each temperature increment. We have used an improved version of the equipment described by Reiss and Michel (1974). The data (temperatures, time-delays, absorbance values), were treated on-line with a NOVA 3D DATA GENERAL computer equipped with graphic outputs, which permitted the absorbance measurements after the time delay required to reach thermal and phase equilibrium in the sample cells. Temperature was measured within ±0.002°C and variations of 10^{-4} A were reproducibly detected. Samples (7 μg DNA/0.5 ml of 0.05 x SSC) were subjected to a stepwise increase in temperature of 0.05°C with a mean delay of 1.5 min per step. Increasing the delay up to 6 min per step did not alter the curves but changes appeared below 1 min (data not shown). Absorbance values are the mean of 256 measurements made at 270 nm at each temperature. At this wavelength the difference in extinction coefficient between AT and GC pairs is negligible (Felsenfeld and Hirshman, 1965).

Quantification of the experimental melting curves, Table I

Curves were smoothed by fitting to a cubic equation over 17 temperature intervals for each experimental value. A program gives the position of the maximum (T_m and Y_m) and the area under the curve which is normalized to the number of bp present in the native fragment. $l_{1/2}$, n_i, $n(T_m)$ and m values are calculated by surface determinations by programs. $l_{1/2}$ is determined graphically. To divide the curves given in Figures 3 and 4 into two thermalites, one determines first the temperature at which d^3A/dT^3 is maximum in the temperature range corresponding to the shoulder. The value corresponding to ΔA_{270} at this temperature yields n_1. By this method, n_1 is underestimated. For the 789-bp curve the temperature associated with the three minima have been taken to define limits between the four thermalites (Figure 5). Absolute $T_{1/2}$ values are reproducible within ±0.3°C. All fragments being dialysed against the same buffer, differences in $T_{1/2}$ (or T_m) are within ±0.02°C. Internal temperature differences in a profile ($T_m - T_{1/2}$, $l_{1/2}$) are within ±0.01°C. Relative error on surface is ±1%.

Quantification of the theoretical curves, Table II

To generate the theoretical curves, we have used the sequence from Dickson *et al.*, 1975) and M. Berman (personal communication) and the variables given in the legend of Figure 5. These curves are analysed as above (cf. Table I) to yield the corresponding parameters.

Acknowledgments

We are greatly indebted to A. Lechien for her help in the preparation of the fragments, to D. Kotlarz for sequencing the 193 bp fragment, to R. Magnier and B. Caudron for the aid in computer programming. We acknowledge M. Katinka and P. Cossart for sequencing advice and S. Busby for helpful suggestions. We thank C. Reiss for his help in the initial development of our melting device. This work was supported by grant MRM 1991 from DGRST and by the CNRS.

References

Backman,K., Ptashne,M., and Gilbert,W. (1976) *Proc. Natl. Acad. Sci. USA*, **73**, 4174-4178.
Benight,A.S., Wartell,R.M., and Howell,D.K. (1981) *Nature*, **289**, 203-205.
Calos,M.P. (1978) *Nature*, **274**, 762-765.
Charnay,P., Perricaudet,M., Galibert,F., and Tiollais,P. (1978) *Nucleic Acids Res.*, **5**, 4479-4494.
Crothers,P.M., Kallenbach,N.R., and Zimm,B.H. (1965) *J. Mol. Biol.*, **11**, 802-820.
Crothers,D.M. (1968) *Biopolymers*, **6**, 1391-1404.
Crothers,D.M., and Zimm,B.H. (1964) *J. Mol. Biol.*, **9**, 1-9.
Dickson,R.C., Abelson,J., Barnes,W.M., and Reznikoff,W.S. (1975) *Science (Wash.)*, **187**, 27-35.
Felsenfeld,G., and Hirshman,S.Z. (1965) *J. Mol. Biol.*, **13**, 407-427.
Hardies,S.C., Hillen,W., Goodman,T.C., and Wells,R.D. (1979) *J. Biol. Chem.*, **254**, 10128-10134.
Hardies,S.C., and Wells,R.D. (1979) *Gene*, **7**, 1-14.

Hillen,W., Goodman,T.C., Benight,A.S., Wartell,R.M., and Wells,R.D. (1981) *J. Biol. Chem.*, **256**, 2761-2766.
Ippen,K., Miller,J.H., Scaife,J., and Beckwith,J. (1968) *Nature*, **217**, 825-827.
Maquat,L.E., and Reznikoff,W.S. (1978) *J. Mol. Biol.*, **125**, 467-490.
Marmur,J., and Doty,P. (1962) *J. Mol. Biol.*, **5**, 109-118.
Maxam,A., and Gilbert,W. (1980) *Methods Enzymol.*, **65**, 499-560.
Miller,J.H. (1972) in *Experiments in Molecular Genetics*, Cold Spring Harbor Laboratory Press, Cold Spring Harbor, NY, p. 48.
Ogata,R., and Gilbert,W. (1977) *Proc. Natl. Acad. Sci. USA*, **74**, 4973-4976.
Patient,R.K., Hardies,S.C., Larson,J.E., Inman,R.B., Maquat,L.E., and Wells,R.D. (1979) *J. Biol. Chem.*, **254**, 5548-5554.
Poland,D., and Scheraga,H.A. (1969) *Biopolymers*, **7**, 887-908.
Reiss,C., and Michel,F. (1974) *Anal. Biochem.*, **62**, 499-508.
Schaeffner,F., Kolb,A., Kotlarz,D., and Buc,H. (1978) *Abstracts of the Sixth International Biophysics Congress*, Kyoto, Japan, p. 394.
Schildkraut,C., and Lifson,S. (1965) *Biopolymers*, **3**, 195-208.
Silverstone,A.E., Arditti,R.R., and Magasanik,B. (1970) *Proc. Natl. Acad. Sci. USA*, **66**, 773-779.
Sturtevant,J.M., Rice,S.A., and Geiduschek,F.P. (1958) *Discussions Faraday Soc.*, **25**, 138-149.
Tiollais,P., Rambach,A., and Buc,H. (1974) *FEBS Lett.*, **48**, 96-100.
Vizard,D., and Ansevin,A.T. (1976) *Biochemistry (Wash.)*, **15**, 741-750.
Wada,A., Yabuki,S., and Husimi,Y. (1980) *CRC Crit. Rev. Biochem.*, **9**, 87-144.